Strong antiferromagnetic correlation effects on the momentum distribution function of the Hubbard model

2009 J. Phys.: Condens. Matter 21 254209

(http://iopscience.iop.org/0953-8984/21/25/254209)

J. Phys.: Condens. Matter **21** (2009) 254209 (6pp) doi:10.1088/0953-8984/21/25/254209

Strong antiferromagnetic correlation effects on the momentum distribution function of the Hubbard model

Adolfo Avella[1,2] **and Ferdinando Mancini**[1]

[1] Dipartimento di Fisica 'E R Caianiello'—Unità CNISM di Salerno, Università degli Studi di Salerno, I-84081 Baronissi (SA), Italy
[2] Laboratorio Regionale SuperMat, CNR-INFM, I-84081 Baronissi (SA), Italy

E-mail: avella@physics.unisa.it

Received 20 March 2009
Published 29 May 2009
Online at stacks.iop.org/JPhysCM/21/254209

Abstract
Strong antiferromagnetic correlations can radically change the behavior of an otherwise paramagnetic system, inducing anomalous effects in the single particle properties and driving the behavior of spin–spin response functions. In order to investigate such physics, we have studied the momentum distribution function of the two-dimensional Hubbard model at low doping, low temperatures and high values of the on-site Coulomb repulsion. The interpretation of the results has greatly benefited from the parallel analysis of the filling, temperature and interaction dependences of the spin–spin correlation function, the antiferromagnetic correlation length and the pole of the spin–spin propagator. On reducing doping or temperature and on increasing the interaction strength, the correlations become stronger and stronger and the Fermi surface develops hole and electron pockets and shows a dual nature (small–large).

(Some figures in this article are in colour only in the electronic version)

1. Introduction

Strong electronic correlations are held responsible for many of the interesting and singular features characterizing novel oxides [1, 2]. In many cases, it is the proximity to an ordered magnetic phase that makes the system behave very anomalously with respect to what we expect in a non-magnetic (paramagnetic) phase [3, 4]. It is very well known that the spin–spin correlations owe their exceptional strength to their electrostatic origin and the mediation of the Pauli principle makes the effects truly quantum and often counterintuitive [5]. For instance, before the advent of high-T_c cuprate superconductors, none would have expected a quite strong Coulomb repulsion ever to be considered the main source of pairing in a system [1, 4]. According to this, we have decided to analyze the dependence of the spin–spin correlations on the external conditions (temperature and filling) and the model parameters (on-site Coulomb repulsion) within the Hubbard model [6–9]. The latter, together with its many extensions and variants, has drawn the attention of condensed matter theorists as it is considered the prototype for strongly correlated systems, but also because it is considered as the minimal model necessary to describe the very fascinating physics of cuprates [10]. At any rate, it is worth mentioning that whether the two-dimensional one-band Hubbard model has long range d-wave pair correlations or not is still an open question. On the one hand, many numerical and analytical studies show clear evidence for d-wave superconductivity in the model [11–29]. On the other hand, there is still numerical work which contests such conclusions [30] (even though the projective character of the numerical procedure used in the analysis does not make the results conclusive) and suggests that Fröhlich and Coulomb long ranged interactions could play an essential role in a realistic model of high-T_c superconductivity [31].

In order to properly capture the many unconventional features revealed by both numerical analysis and experiments (we adopt the deep-rooted belief that Hubbard model $\equiv$ cuprates), we have decided to use the composite operator method with the residual self-energy computed in the non-crossing approximation [COM(NCA)] [32, 33]. COM is a theoretical formulation that is completely microscopic, exclusively analytical and fully self-consistent. The COM recipe uses three main ingredients: composite

operators, algebra constraints and residual self-energy treatment. Composite operators are products of electronic operators and describe the new elementary excitations appearing in the system owing to strong correlations. Algebraic constraints are relations among correlation functions dictated by the noncanonical operatorial algebra satisfied by the chosen operatorial basis. The residual self-energy, i.e. the propagator of the residual term of the current after this latter has been projected on the basis, describes the interactions among the composite operators.

2. Model and method

The Hamiltonian of the two-dimensional Hubbard model reads as

$$H = \sum_{\mathbf{ij}} \left(-\mu\delta_{\mathbf{ij}} - 4t\alpha_{\mathbf{ij}}\right) c^{\dagger}(i)c(j) + U\sum_{\mathbf{i}} n_{\uparrow}(i)n_{\downarrow}(i) \quad (1)$$

where

$$c(i) = \begin{pmatrix} c_{\uparrow}(i) \\ c_{\downarrow}(i) \end{pmatrix} \quad (2)$$

is the electron field operator in spinorial notation and the Heisenberg picture ($i = (\mathbf{i}, t_i)$), $\mathbf{i} = \mathbf{R_i}$ is a vector of the Bravais lattice, $n_{\sigma}(i) = c^{\dagger}_{\sigma}(i)c_{\sigma}(i)$ is the particle density operator for spin σ, $n(i) = \sum_{\sigma} n_{\sigma}(i)$ is the total particle density operator, μ is the chemical potential, t is the hopping integral and the energy unit, U is the Coulomb on-site repulsion and $\alpha_{\mathbf{ij}}$ is the projector on the nearest-neighbor sites

$$\alpha_{\mathbf{ij}} = \frac{1}{N}\sum_{\mathbf{k}} \mathrm{e}^{\mathrm{i}\mathbf{k}\cdot(\mathbf{R_i}-\mathbf{R_j})}\alpha(\mathbf{k})$$
$$\alpha(\mathbf{k}) = \tfrac{1}{2}\left[\cos(k_x a) + \cos(k_y a)\right] \quad (3)$$

where $\mathbf{k}$ runs over the first Brillouin zone, N is the number of sites and a is the lattice constant. We will often use the following notation:

$$\psi^{\alpha}(\mathbf{i}) = \sum_{\mathbf{j}} \alpha_{\mathbf{ij}}\psi(\mathbf{j}). \quad (4)$$

Following COM prescriptions [32], we have chosen as the operatorial basis

$$\psi(i) = \begin{pmatrix} \xi(i) \\ \eta(i) \end{pmatrix} \quad (5)$$

with $\eta(i) = n(i)c(i)$ and $\xi(i) = c(i) - \eta(i)$, guided by the hierarchy of the equations of motion and by the exact solution of the Hubbard Hamiltonian reduced to its interacting term. Until further notice, all objects appearing in the equations stand for two by two matrices, according to the vectorial nature of the operatorial basis.

The field $\psi(i)$ satisfies the following equation of motion:

$$\mathrm{i}\frac{\partial}{\partial t}\psi(i) = \sum_{\mathbf{j}} \varepsilon_{\mathbf{ij}}\psi(\mathbf{j}, t) + \delta J(i) \quad (6)$$

where the energy matrix $\varepsilon_{\mathbf{ij}}$ is defined after the request that the residual current $\delta J(i)$ satisfies the constraint $\langle\{\delta J(\mathbf{i}, t), \psi^{\dagger}(\mathbf{j}, t)\}\rangle = 0$. This constraint ensures that the residual current $\delta J(i)$ describes the physics *orthogonal* to the chosen operatorial basis $\psi(i)$; that is, $\delta J(i)$ describes the interactions among the elements of the operatorial basis. According to this, the Fourier transform of the energy matrix $\varepsilon(\mathbf{k})$ reads as

$$\varepsilon(\mathbf{k}) = \tilde{\varepsilon} - 4t\left\{\alpha(\mathbf{k})I\,(1+\sigma_1) + \left[\alpha(\mathbf{k})p + \Delta\right](1-\sigma_1)\,I^{-1}\right\} \quad (7)$$

where

$$\tilde{\varepsilon} = \begin{pmatrix} -\mu & 0 \\ 0 & U-\mu \end{pmatrix} \quad (8)$$

$$\Delta = \left\langle\xi^{\alpha}(i)\xi^{\dagger}(i)\right\rangle - \left\langle\eta^{\alpha}(i)\eta^{\dagger}(i)\right\rangle \quad (9)$$

is the difference between upper and lower intra-subband contributions to the kinetic energy and

$$p = \tfrac{1}{4}\left\langle\delta n^{\alpha}_{\mu}(i)\delta n_{\mu}(i)\right\rangle - \left\langle\left[c_{\uparrow}(i)c_{\downarrow}(i)\right]^{\alpha} c^{\dagger}_{\downarrow}(i)c^{\dagger}_{\uparrow}(i)\right\rangle \quad (10)$$

is a combination of the nearest-neighbor charge–charge, spin–spin and pair–pair correlation functions. $\delta n_{\mu}(i) = n_{\mu}(i) - \langle n_{\mu}(i)\rangle$ stands for charge ($n_0(i) = n(i)$) and spin ($n_k(i) = c^{\dagger}(i)\sigma_k c(i)$ $k = 1, 2, 3$) number operators and the sum over repeated indices is understood. $\sigma_{\mu} = (1, \sigma_k)$, $\sigma^{\mu} = (-1, \sigma_k)$ and σ_k are the Pauli matrices.

The Fourier transform of the normalization matrix $I = \mathcal{F}\langle\{\psi(\mathbf{i}, t), \psi^{\dagger}(\mathbf{j}, t)\}\rangle$ reads as

$$I = \begin{pmatrix} 1 - \frac{n}{2} & 0 \\ 0 & \frac{n}{2} \end{pmatrix} \quad (11)$$

where n is the filling and $\mathcal{F}$ stands for the Fourier transform operator.

After the equation of motion satisfied by $\psi(i)$, the Fourier transform of the retarded Green's function $G(i, j) = \langle R[\psi(i)\psi^{\dagger}(j)]\rangle$ has the following expression:

$$G(\mathbf{k}, \omega) = \frac{1}{\omega - \varepsilon(\mathbf{k}) - \Sigma(\mathbf{k}, \omega)I^{-1}}I \quad (12)$$

where $\Sigma(\mathbf{k}, \omega) = \mathcal{F}\langle R[\delta J(i)\delta J^{\dagger}(j)]\rangle_{\mathrm{irr}}$ is the residual self-energy. The subscript irr denotes the irreducible part of the propagator.

By exploiting algebraic constraints [32] and connections between propagators and correlators, we fix the parameters appearing in the energy matrix $\varepsilon(\mathbf{k})$ (μ, Δ, and p) through a set of three self-consistent equations

$$n = 2(1 - C_{11} - 2C_{12} - C_{22}) \quad (13)$$

$$\Delta = C^{\alpha}_{11} - C^{\alpha}_{22} \quad (14)$$

$$C_{12} = 0 \quad (15)$$

where $C_{ab} = \langle\psi_a(i)\psi^{\dagger}_b(i)\rangle$ and $C^{\alpha}_{ab} = \langle\psi^{\alpha}_a(i)\psi^{\dagger}_b(i)\rangle$. The first two equations are obtained by expressing the filling n and the parameter Δ in terms of correlators. The third equation is the algebraic constraint $\langle\xi(i)\eta^{\dagger}(i)\rangle = 0$ that excludes double occupancy of a site by two electrons with the same spin.

We have chosen to compute the residual self-energy $\Sigma(\mathbf{k}, \omega)$ within the NCA [32–35]. First, we have rewritten $\delta J(i)$ in terms of the charge, spin and electronic fields,

discarding the pair field $c_\uparrow(i)c_\downarrow(i)$ and the *reducible* contributions

$$\delta J(i) \approx \tfrac{1}{2}\sigma^\mu \delta n_\mu(i) c^\alpha(i) \begin{pmatrix} 1 \\ -1 \end{pmatrix}. \tag{16}$$

According to this, the residual self-energy reads as

$$\Sigma(\mathbf{k},\omega) = 4t^2 \mathcal{F}\left\langle R\left[\sigma^\mu \delta n_\mu(i) c^\alpha(i) c^{\dagger\alpha}(j) \sigma^\mu \delta n_\mu(j)\right]\right\rangle \times (1-\sigma_1). \tag{17}$$

Then, by *mode-decoupling* the corresponding causal Green's function

$$\left\langle T\left[\sigma^\mu \delta n_\mu(i) c^\alpha(i) c^{\dagger\alpha}(j) \sigma^\mu \delta n_\mu(j)\right]\right\rangle \approx \left\langle T\left[\delta n_\mu(i)\delta n_\mu(j)\right]\right\rangle \left\langle T\left[c^\alpha(i) c^{\dagger\alpha}(j)\right]\right\rangle \tag{18}$$

the residual self-energy $\Sigma(\mathbf{k},\omega)$ can be approximated as follows:

$$\Sigma(\mathbf{k},\omega) = 4t^2 \mathcal{F}_\mathbf{k}\left[S(\mathbf{r},\omega)\right](1-\sigma_1) \tag{19}$$

where

$$S(\mathbf{r},\omega) = \int\int \frac{\mathrm{d}\omega' \mathrm{d}\Omega}{(2\pi)^2} \frac{1+\mathrm{e}^{-\beta\omega'}}{\omega-\omega'+\mathrm{i}\varepsilon} F(\mathbf{r},\Omega) B(\mathbf{r},\omega'-\Omega). \tag{20}$$

The two propagators F and B are defined as follows:

$$F(\mathbf{i}-\mathbf{j},\omega) = \mathcal{F}_\omega\left\langle c^\alpha(i) c^{\dagger\alpha}(j)\right\rangle \tag{21}$$

and

$$B(\mathbf{i}-\mathbf{j},\omega) = \mathcal{F}_\omega\left\langle \delta n_\mu(i)\delta n_\mu(j)\right\rangle. \tag{22}$$

$\mathcal{F}_\omega$ and $\mathcal{F}_\mathbf{k}$ stand for the time–frequency and position–momentum Fourier transform operators, respectively.

Within the NCA, the residual self-energy Σ is expressed as the convolution of the bosonic propagators B and of the fermionic propagator F. This latter can be computed in terms of the Green's function G, whereas the former can be self-consistently computed in the two-pole approximation. In fact, instead of using a phenomenological expression for the spin susceptibility and neglecting the charge susceptibility, as in [36–38], we have analytically computed both charge and spin propagators. This procedure has the great advantage of allowing a self-consistent determination of the doping and temperature dependences of the correlation lengths and eliminates the need for any numerical estimate of them.

We have chosen to use the two-pole approximation that has been shown to be capable of catching many important features [32, 39, 40]. Within this approach, we have chosen as a basis

$$\psi_\mu(i) = \begin{pmatrix} \delta n_\mu(i) \\ \rho_\mu(i) \end{pmatrix} \tag{23}$$

where

$$\rho_\mu(i) = c^\dagger(i)\sigma_\mu c^\alpha(i) - c^{\dagger\alpha}(i)\sigma_\mu c(i) \tag{24}$$

is the new composite operator appearing in the current of the operator $\delta n_\mu(i)$.

The field $\psi_\mu(i)$ satisfies the following equation of motion:

$$\mathrm{i}\frac{\partial}{\partial t}\psi_\mu(i) = \sum_\mathbf{j} \varepsilon_{\mu\mathbf{ij}}\psi_\mu(\mathbf{j},t) + \delta J_\mu(i) \tag{25}$$

where the energy matrix $\varepsilon_{\mu\mathbf{ij}}$ is defined after the request that the residual current $\delta J_\mu(i)$ satisfies the constraint $\langle[\delta J_\mu(\mathbf{i},t), \psi^\dagger_\mu(\mathbf{j},t)]\rangle = 0$. The energy matrix $\varepsilon_{\mu\mathbf{ij}}$ and the normalization matrix $I_\mu(\mathbf{i}-\mathbf{j}) = \langle[\psi_\mu(\mathbf{i},t), \psi^\dagger_\mu(\mathbf{j},t)]\rangle$ depend on both electronic correlators

$$C_{ab}(\mathbf{i}-\mathbf{j}) = \left\langle \psi_a(\mathbf{i})\psi^\dagger_b(\mathbf{j})\right\rangle \tag{26}$$

and high-order (with respect to the chosen operatorial basis) charge and spin correlation functions a_μ, b_μ, c_μ, and d_μ [32, 39]. By means of the hydrodynamics constraint [32, 39], we can fix the greatest part of the unknowns. The two remaining parameters a_c and a_s, one per channel, can be fixed through the algebraic constraints

$$\langle n(i)n(i)\rangle = n + 2D \tag{27}$$

$$\langle n_z(i)n_z(i)\rangle = n - 2D \tag{28}$$

where $D = \langle n_\uparrow(i)n_\downarrow(i)\rangle = n/2 - C_{22}$ is the double occupancy. Equation (27) excludes double occupancy of a site by two electrons with the same spin and equation (28) enforces the relation between filling and *length* of the electronic spin on the same site.

After the equation of motion satisfied by $\psi_\mu(i)$, the Fourier transform of the retarded Green's function $G_\mu(i,j) = \langle R[\psi_\mu(i)\psi^\dagger_\mu(j)]\rangle$ has the following expression in the two-pole approximation (i.e. by neglecting $\delta J_\mu(i)$):

$$G_\mu(\mathbf{k},\omega) = \frac{1}{\omega - \varepsilon_\mu(\mathbf{k})} I_\mu(\mathbf{k}). \tag{29}$$

In conclusion, we can compute $B(i,j)$, necessary to determine the residual self-energy $\Sigma(\mathbf{k},\omega)$ within the NCA, as

$$B(i,j) = \sum_{\mu=0}^{3} G_{\mu 11}(i,j). \tag{30}$$

3. Results

In the following, we present some results by considering the momentum distribution function per spin

$$n(\mathbf{k}) = -\frac{1}{\pi}\int \mathrm{d}\omega\, f_\mathrm{F}(\omega)\,\mathrm{Im}\left[G(\mathbf{k},\omega)\right], \tag{31}$$

the spin–spin correlation function $\langle n_z n_z^\alpha\rangle$, the pole $\varepsilon_s(\mathbf{Q})$ of the spin–spin propagator and the antiferromagnetic correlation length ξ. The latter is usually defined by supposing the following asymptotic expression for the static susceptibility:

$$\lim_{\mathbf{k}\to\mathbf{Q}} \chi_\mathrm{s}(\mathbf{k},0) = \frac{\chi_\mathrm{s}(\mathbf{Q},0)}{1+\xi^2|\mathbf{k}-\mathbf{Q}|^2} \tag{32}$$

where $\chi_\mathrm{s}(\mathbf{k},0) = -G_\mathrm{s}(\mathbf{k},0)$. It is worth noting that equation (32) exactly holds in our case [40].

In figure 1, we present the spin–spin correlation function $\langle n_z n_z^\alpha\rangle$, the antiferromagnetic correlation length ξ and the pole $\omega(\mathbf{Q}) = \varepsilon_s(\mathbf{Q})$ as functions of filling n, temperature T and on-site Coulomb repulsion U for values in the ranges

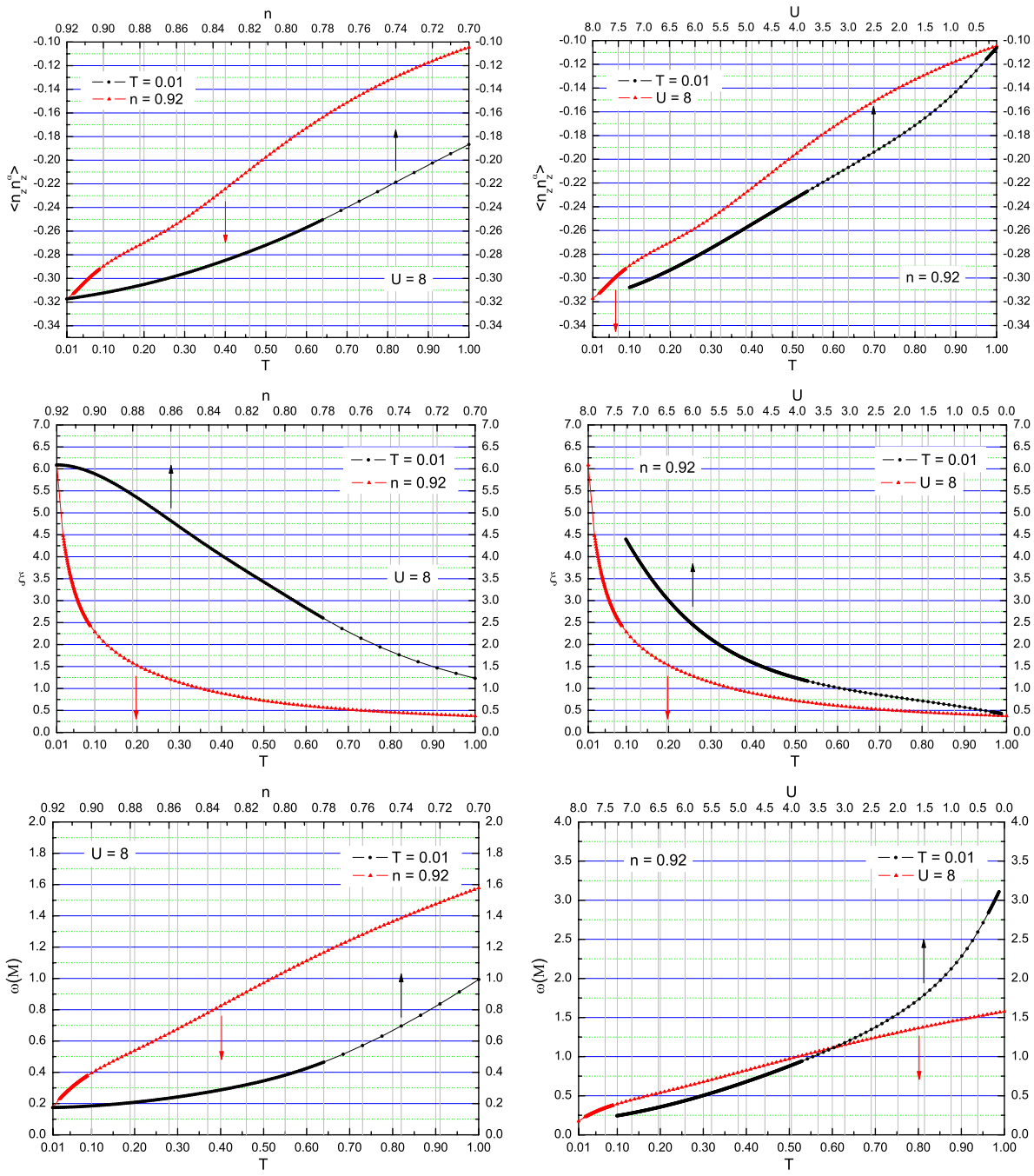

Figure 1. The spin–spin correlation function $\langle n_z n_z^\alpha \rangle$, the pole $\omega(\mathbf{Q})$ of the spin–spin propagator and the antiferromagnetic correlation length ξ as functions of filling n, temperature T and on-site Coulomb repulsion U in the ranges $0.7 < n < 0.92$, $0.01 < T < 1$ and $0.1 < U < 8$.

$0.7 < n < 0.92$, $0.01 < T < 1$ and $0.1 < U < 8$. We wish to analyze the behavior of these quantities as the parameters reach the extremal values $n = 0.92$, $T = 0.01$ and $U = 8$, where we have already shown that the single particle properties (spectral density function, Fermi surface, dispersion relation, density of states, momentum distribution function) present anomalous behaviors qualitatively similar to what has been found in underdoped cuprates [33]. The spin–spin correlation function $\langle n_z n_z^\alpha \rangle$ is always antiferromagnetic (negative) and increases its absolute value on decreasing doping and temperature T and on increasing U. It is evident the signature of the scale of energy of $J \approx \frac{4t^2}{U} \approx 0.5$ in the temperature dependence as a significant enhancement in the slope. The filling dependence shows quite strong correlations at the higher dopings too. The antiferromagnetic correlation length ξ overcomes one lattice constant at temperatures below J and tends to diverge for low enough temperatures. ξ is always larger than 1 for all values of fillings, showing that, at $T = 0.01$ and $U = 8$, we should expect quite well defined antiferromagnetic fluctuations also in the overdoped regime. On the other hand, ξ seems to saturate for low enough dopings. ξ equals 1 between $U = 3$ and 4 and again rapidly increases for large enough values of U. The

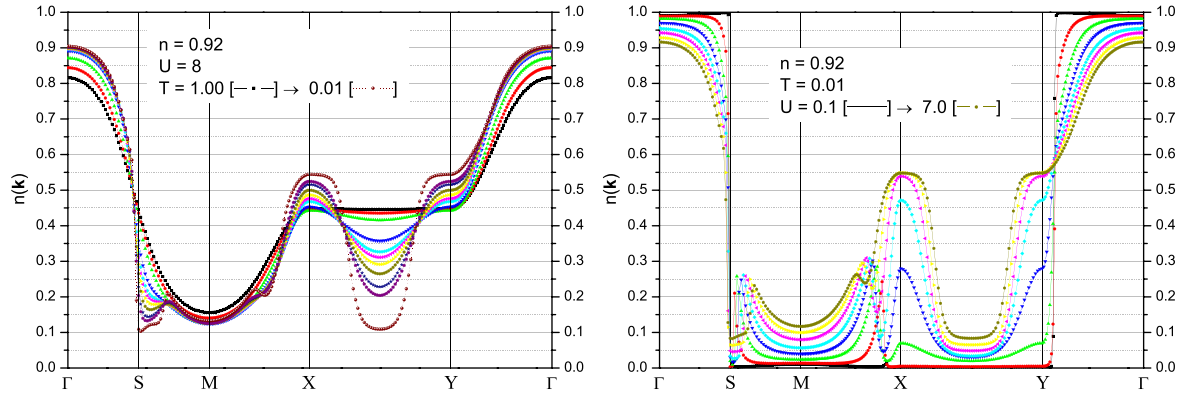

Figure 2. The momentum distribution function $n(\mathbf{k})$ along the main directions ($\Gamma = (0, 0) \rightarrow M = (\pi, \pi) \rightarrow X = (\pi, 0) \rightarrow Y = (0, \pi) \rightarrow \Gamma = (0, 0)$) for different values of temperature T and on-site Coulomb repulsion U at $n = 0.92$.

pole $\omega(\mathbf{Q})$ decreases on decreasing doping n and temperature T and on increasing U. In particular, it is very sensitive to the variations in temperature T and on-site Coulomb repulsion U, making the mode softer and softer and clearly showing the definite tendency to the antiferromagnetic phase.

In figure 2, we report the momentum distribution function $n(\mathbf{k})$ along the main directions ($\Gamma = (0, 0) \rightarrow M = (\pi, \pi) \rightarrow X = (\pi, 0) \rightarrow Y = (0, \pi) \rightarrow \Gamma = (0, 0)$) for different values of temperature T and on-site Coulomb repulsion U at $n = 0.92$. Down to $T = 0.4$ (up triangles), the behavior is that of a correlated paramagnet. For lower temperatures, a hole pocket develops along the main diagonal $\Gamma \rightarrow M$ in the proximity of $S = (\pi/2, \pi/2)$ and electron pockets form at X and Y. Such a behavior is what one expects when quite strong magnetic fluctuations develop in the system, and corresponds to a well defined tendency towards an antiferromagnetic phase. The M point becomes another minimum in the dispersion in competition with Γ and the dispersion should present a maximum between them corresponding to the center of the hole pocket. The whole bending of the dispersion confines the van Hove singularity below the Fermi surface in an electron pocket visible in the momentum distribution as a new quite broad maximum at X and Y. The dependence on U shows that for $n = 0.92$ and $T = 0.01$, our solution presents quite strong antiferromagnetic fluctuations for every finite value of the Coulomb repulsion, although the pockets (both hole and electron) are not well formed for values of U less than $U =$ 3–4. It is worth noticing that, along the main diagonal, the point $n(\mathbf{k}) = 0.5$ is a fixed point for all temperatures and that the hole pocket has a fixed border at S showing quite an interesting behavior with Fermi liquid features within the magnetic zone and non-Fermi liquid ones outside of it.

In figure 3, we try to summarize the scenario in the extreme case ($n = 0.92$, $T = 0.01$ and $U = 8$), where all the anomalous features are present and well formed, by reporting the full 2D scan of the momentum distribution function $n(\mathbf{k})$ in a quarter of the Brillouin zone. The dotted line is a guide to the eye and marks the reduced (antiferromagnetic) Brillouin zone. The dashed–dotted line gives the position of the level $n(\mathbf{k}) = 0.5$ and can be used as reference for an ordinary Fermi

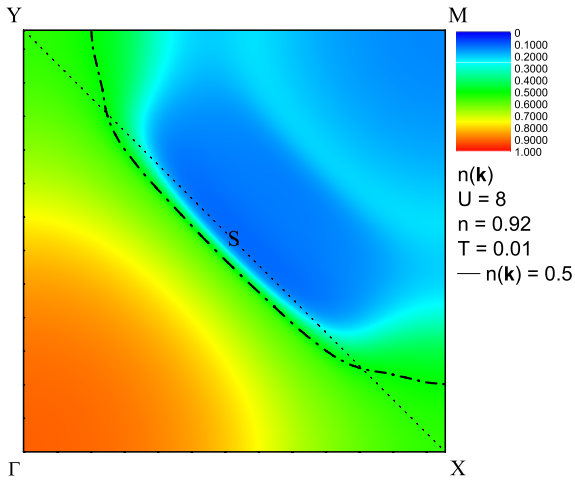

Figure 3. The momentum distribution function $n(\mathbf{k})$ for $n = 0.92$, $T = 0.01$ and $U = 8$.

liquid, although this is clearly not the case. We can clearly see now the hole pocket with its center along the main diagonal and the lower border touching the border of the magnetic zone at exactly $S = (\pi/2, \pi/2)$. Actually, the 2D perspective makes it more evident that there is a second underlying Fermi surface that corresponds to the ordinary paramagnetic one for this filling $n = 0.92$ (large and hole-like) and touching the border of the zone between $M = (\pi, \pi)$ and $X = (\pi, 0)$ ($Y = (0, \pi)$). This corresponds to the very small jump in figure 2 (left panel) along the same direction. Such a behavior can be relevant for solving the old dichotomy arising by the simultaneous presence of a large Fermi surface and of a small one that is proper for heavy-fermions physics.

4. Conclusions

We have studied the effects of strong antiferromagnetic correlations on the momentum distribution function $n(\mathbf{k})$ of the Hubbard model on varying filling, temperature and value of on-site Coulomb repulsion U. In order to properly

interpret the behavior of $n(\mathbf{k})$, we have also analyzed the characteristic features in the spin–spin correlation function, the antiferromagnetic correlation length and the pole of the spin–spin propagator. In the extreme case ($n = 0.92$, $T = 0.01$ and $U = 8$), hole and electron pockets develop. Two Fermi surface branches are visible: one small one defined by the hole pocket centered on the main diagonal of the Brillouin zone and touching the border of the magnetic zone at S and one large and hole-like one touching the border of the zone between M and $X(Y)$. On reducing doping or temperature and on increasing U, the correlations become stronger and stronger. The scale of energy of J is clearly visible in the temperature dependence of the spin–spin correlation function $\langle n_z n_z^{\alpha} \rangle$.

References

[1] Dagotto E 1994 *Rev. Mod. Phys.* **66** 763
[2] Georges A, Kotliar G, Krauth W and Rozenberg M J 1996 *Rev. Mod. Phys.* **68** 13
[3] Imada M, Fujimori A and Tokura Y 1998 *Rev. Mod. Phys.* **70** 1039
[4] Lee P A, Nagaosa N and Wen X-G 2006 Doping a mott insulator: physics of high-temperature superconductivity *Rev. Mod. Phys.* **78** 17
[5] Ashcroft N W and Mermin D N 1976 *Solid State Physics* (Toronto: Thomson Learning)
[6] Hubbard J 1963 *Proc. R. Soc.* A **276** 238
[7] Hubbard J 1964 *Proc. R. Soc.* A **277** 237
[8] Hubbard J 1964 *Proc. R. Soc.* A **281** 401
[9] Hubbard J 1965 *Proc. R. Soc.* A **285** 542
[10] Anderson P W 1987 *Science* **235** 1196
[11] Bickers N E, Scalapino D J and White S R 1989 *Phys. Rev. Lett.* **62** 961
[12] Scalapino D J 1995 *Phys. Rep.* **250** 329
[13] Avella A, Mancini F, Villani D and Matsumoto H 1997 The superconducting gap in the two-dimensional Hubbard model *Physica* C **282** 1757
[14] Di Matteo T, Mancini F, Matsumoto H and Oudovenko V S 1997 Singlet pairing in the 2D Hubbard model *Physica* B **230** 915
[15] Carbotte J, Schachinger E and Basov D 1999 *Nature* **401** 354
[16] Jarrell M *et al* 2001 *Phys. Rev.* B **64** 195130
[17] Moriya T and Ueda K 2003 *Rep. Prog. Phys.* **66** 1299
[18] Snchal D, Lavertu P-L, Marois M-A and Tremblay A-M S 2005 *Phys. Rev. Lett.* **94** 156404
[19] Maier T A, Jarrell M, Schulthess T C, Kent P R C and White J B 2005 *Phys. Rev. Lett.* **95** 237001
[20] Kancharla S, Civelli M, Capone M, Kyung B, Snchal D, Kotliar G and Tremblay A-M S 2005 arXiv:cond-mat/0508205
[21] Tremblay A-M S, Kyung B and Sénéchal D 2006 Pseudogap and high-temperature superconductivity from weak to strong coupling. towards quantitative theory *Fiz. Nizk. Temp.* **32** 561
Tremblay A-M S, Kyung B and Sénéchal D 2006 *Low Temp. Phys.* **32** 424
[22] Nickel J C, Duprat R, Bourbonnais C and Dupuis N 2006 *Phys. Rev.* B **73** 165126
[23] Haule K and Kotliar G 2007 *Phys. Rev.* B **76** 104509
[24] Reiss J, Rohe D and Metzner W 2007 *Phys. Rev.* B **75** 075110
[25] Edegger B, Muthukumar V and Gros C 2007 *Adv. Phys.* **56** 927
[26] Spanu L, Lugas M, Becca F and Sorella S 2008 *Phys. Rev.* B **77** 024510
[27] Hassan S R, Davoudi B, Kyung B and Tremblay A-M S 2008 *Phys. Rev.* B **77** 094501
[28] Tsai W-F, Yao H, Luchli A and Kivelson S A 2008 *Phys. Rev.* B **77** 214502
[29] Lee P 2008 *Rep. Prog. Phys.* **71** 012501
[30] Aimi T and Imada M 2007 *J. Phys. Soc. Japan* **76** 113708
[31] Alexandrov A S and Kornilovitch P E 2002 *J. Phys.: Condens. Matter* **14** 5337
[32] Mancini F and Avella A 2004 The Hubbard model within the equations of motion approach *Adv. Phys.* **53** 537
[33] Avella A and Mancini F 2007 Underdoped cuprates phenomenology in the 2d Hubbard model *Phys. Rev.* B **75** 134518
[34] Avella A, Krivenko S, Mancini F and Plakida N M 2004 Self-energy corrections to the electronic spectrum of the Hubbard model *J. Magn. Magn. Mater.* **272** 456
[35] Krivenko S, Avella A, Mancini F and Plakida N 2005 SCBA within composite operator method for the Hubbard model *Physica* B **359** 666
[36] Chubukov A V and Norman M R 2004 Dispersion anomalies in cuprate superconductors *Phys. Rev.* B **70** 174505 and references therein
[37] Prelovšek P and Ramšak A 2005 Spin-fluctuation mechanism of superconductivity in cuprates *Phys. Rev.* B **72** 012510
[38] Plakida N M and Oudovenko V S 2007 Electron spectrum of high-temperature cuprate superconductors *JETP* **104** 230
[39] Avella A, Mancini F and Turkowski V 2003 Bosonic sector of the two-dimensional Hubbard model studied within a two-pole approximation *Phys. Rev.* B **67** 115123
[40] Avella A and Mancini F 2003 A theoretical analysis of the magnetic properties of LaCuO *Eur. Phys. J.* B **32** 27